Applied Clay Science 139 (2017) 92–98

Contents lists available at ScienceDirect

Applied Clay Science

journal homepage: www.elsevier.com/locate/clay

Research paper

Removal of manganese (II) by edge site adsorption on raw and milled vermiculites

B. Kebabi [a], S. Terchi [a,b], H. Bougherara [a], L. Reinert [b], L. Duclaux [b,*]

[a] Laboratoire Pollution et Traitement des Eaux, Département de Chimie, Université Mentouri, 25000 Constantine, Algeria
[b] Université Savoie Mont Blanc, LCME, 73000 Chambéry, France

ARTICLE INFO

Article history:
Received 16 August 2016
Received in revised form 26 December 2016
Accepted 28 December 2016
Available online 26 January 2017

Keywords:
Manganese
Adsorption
Vermiculite
Layer edge
Exchange
Sonication

ABSTRACT

The adsorption mechanism of manganese nitrate on vermiculite was studied by analysis of the isotherms of the cations exchanged from the vermiculite (K^+ and Ca^{2+}) and the ions (NO_3^- and Mn^{2+}) adsorbed on the vermiculite. The Langmuir-type manganese adsorption isotherm of the raw vermiculite shows a maximum uptake of 28.32 $mg \cdot g^{-1}$. The adsorption temperature dependence between 25 °C and 45 °C has demonstrated an endothermic and spontaneous adsorption. The amount of exchanged Mn^{2+} ions in equivalent per gram represents only 17% of the total adsorbed uptake, of which 14% have been exchanged against Ca^{2+} ions and 3% against K^+ ions. 83% of the Mn^{2+} and NO_3^- ions have been co-adsorbed by complexation at the edges of the layers. The grinding of the vermiculite has involved a decrease in the grains size from 2–3 mm to 100 μm and thus an increase in the edge layer adsorption site content allowing an increase of 19% of the maximum adsorption uptake compared to raw vermiculite. The ultrasonic milling of vermiculite in aqueous dispersion at 20 kHz allowed to decrease the size of the grains further (8 μm) and led to increase the maximum uptake by 31%. The sonication of the vermiculite dispersion in 35% hydrogen peroxide has allowed to obtain a maximum adsorption uptake of 36.77 $mg \cdot g^{-1}$ (30% of increase compared to raw vermiculite). The linear variation of the Mn^{2+} adsorption capacity with respect to the sum of the estimated geometric perimeter of the sonicated particles (assuming square shaped particles) confirms an adsorption process at the edge of layers.

1. Introduction

Among the heavy metals, manganese is a contaminant of wastewater and ground water because of its use as industrial raw material. Part of the manganese issued from the human activities, e.g. from the production of manganese steels (Krauss, 2005), ferro-manganese alloys (Olsen et al., 2007) or methylcyclopentadienyl manganese tricarbonyl (MMT) (Pfeifer et al., 2004), may attain the water resources. The World Health Organization recommends a maximum manganese content in drinking water of 0.4 $mg \cdot L^{-1}$ (WHO, 2011). The main European countries have a standard of 0.05 $mg \cdot L^{-1}$ or below. Many techniques can be used for the removal of manganese from water such as precipitation, coagulation/flocculation, ion exchange, oxidation–filtration, electrochemical or biological operations, adsorption and membrane processes (Patil et al., 2016). Among them, adsorption is a low-cost effective method to remove this element. A lot of adsorbents with various adsorption uptakes can be used for the removal of manganese: activated carbons (Jusoh et al., 2005), minerals such as metal oxides (Hua et al., 2012) or zeolites (Ates and Akgül, 2016), biomass (Spinti et al., 1995), polymers, etc.

In the recent review of Patil et al. (Patil et al., 2016), the comparison of the Mn^{2+} adsorption capacities of various adsorbents has shown that some clay minerals are among the materials with the highest uptakes. As for example, a Mn^{2+} uptake of ~111 $mg \cdot g^{-1}$ was measured for a kaolinite (Dawodu and Akpomie, 2014) and for an alkaline modified montmorillonite (Akpomie and Dawodu, 2014). Particularly, the smectites are interesting materials because they can retain the Mn^{2+} cations by ionic exchange or by formation of inner–sphere complexes at the edges of the layers.

In this present work, the vermiculite was selected for its strong adsorption capacity related to its high layers' charge, its cationic exchange properties (120–150 meq/100 g), its chemical inertness and environmental safety (Lagaly et al., 2006; Valaškova and Simha Martynkova, 2012). Previous researches have been devoted to the removal of manganese using vermiculites. Recently, Malandrino et al. (2006) demonstrated that this mineral presents good potential for cost-effective treatments of metal-contaminated wastewaters. Particularly, they reported the highest total adsorption capacity of vermiculite for Mn^{2+} (97.5 meq/100 g corresponding to 26.8 $mg \cdot g^{-1}$) and showed that the affinity for the metallic ions decreased in the following order:

* Corresponding author.
E-mail address: laurent.duclaux@univ-smb.fr (L. Duclaux).

http://dx.doi.org/10.1016/j.clay.2016.12.041
0169-1317/

Mn > Ni > Zn > Cd > Cu > Pb. They also reported that the adsorption of metallic ions on vermiculite decreases with the pH decrease and the ionic strength increase.

Da Fonseca et al. (2006) have reported the use of vermiculite to remove manganese from aqueous solutions of manganese nitrate and obtained a maximum uptake of 33 $mg \cdot g^{-1}$ at pH higher than 6.4. They reported Langmuir type isotherms and claimed that the adsorption was mainly governed by ionic exchange at pH lower than 9 but they didn't measure the concentration of released exchangeable cations. These authors have proposed that at pH higher than 9, Mn^{2+} removal could occur by two mechanisms: cationic hydroxo complexes adsorption and $Mn^{n+}(OH)_n$ precipitation on the vermiculite surface.

These preceding studies focused on the mechanism of adsorption of Mn^{2+} cations on vermiculite, and did not discuss the role of cationic exchange and complexation separately.

Previous work on the adsorption of boron by sonicated vermiculites has demonstrated that the reduction of the size of the particles, without degradation of the vermiculite structure, could improve its adsorption capacity (Kehal et al., 2010). Numerous studies have examined the use of a sonication process to delaminate the vermiculite layers, in order to obtain submicron and micron size particles (Jimenez de Haro et al., 2004; Nguyen et al., 2013; Pérez-Maqueda et al., 2001; Perez-Rodriguez et al., 2002; Poyato et al., 2009; Wiewiora et al., 2003). Ali et al. (2014) have studied the effect of sonication conditions (solvent, time, temperature and reactor type) on the preparation of micron size vermiculite particles. Ultrasound irradiation was reported to avoid undesirable crystal structure damage as compared to grinding, because the long range order is almost unaffected by sonication (Pérez-Maqueda et al., 2004; Perez-Rodriguez et al., 2002). Reinholdt et al. (2013) have shown that different size fractions obtained by sonication can be selected by using a combination of different methods: wet sieving, centrifugation and settling. More recently, Dzene et al. (2015) have observed that the amount of desorbed cesium after its adsorption on a Na-vermiculite is correlated to the ratio between external sites (basal external sites and edge sites) and the total number of sites present on vermiculite. The highest proportion of desorbed cesium ($34 \pm 7\%$ of the initially adsorbed Cs^+) has been found for the smallest size fraction (0.1–0.2 μm) for which the sonication has generated the highest amount of external sites. This latter work has confirmed that sonication can greatly improve the external adsorption, particularly by increasing the number of edge sites.

The objectives of the present work are the determination of the Mn^{2+} cations adsorption mechanism on raw and milled vermiculites. In order to determine both the amount of Mn^{2+} exchanged cations and complexed ones (at the edge of the layers), the isotherms of the exchangeable cations from the vermiculite (K^+ and Ca^{2+}) and the adsorbed ions (NO_3^- and Mn^{2+}) on the vermiculite were investigated. The conventional and ultrasound milling was used for decreasing the particle size and thus increasing the number of edge sites.

2. Materials and methods

2.1. The adsorbents

The vermiculite adsorbent used in this study, originating from Yuli (China), was purchased from CMMP (Paris, France). Before its use, it was washed several times with distilled water and dried at 105 °C for 12 h. The average particle size of the raw vermiculite is 2–3 mm.

The average chemical composition of the half lattice cell, calculated from elemental analysis (i.e., $(Si_3Al_1)(Mg_{2.62}Fe_{0.32}Ti_{0.06})O_{10}(OH)_2K_{0.45}Ca_{0.08}$, Nguyen et al., 2013) indicates that the exchangeable ions are either potassium or calcium.

A mechanical milling (using a mixer) has allowed reducing the particle size to about 100 μm; the obtained sample was referred to milled vermiculite. 7 g of this milled vermiculite were agitated in 100 mL of a 35 mass % hydrogen peroxide solution for 5 h for a chemical exfoliation, and then filtered off and dried for 48 h in an oven at 80 °C. The obtained sample was referred to "H_2O_2 vermiculite". The size reduction of vermiculite without modification of its structure (Reinholdt et al., 2013) was obtained by sonication of the milled vermiculite (3.85 g) at 20 kHz using a probe (Ultrasonic Processor-VC505, Sonics and Materials, 80 μm amplitude, 13 mm diameter) immersed (1.5 cm depth) in 55 mL of dispersion maintained at 25 °C in a cylindrical glass double-jacketed reactor that was cooled by a circulating cryostat. The dispersions were prepared either in pure water or in a 35 mass % hydrogen peroxide aqueous solution. In such conditions, the vermiculite percentage in the dispersion was of 6.5 mass %. The sonication times were set to 2 or 5 h. After sonication, the dispersions were filtered off and the solids were dried in an oven at 105 °C for 12 h. The samples sonicated in pure water for 2 h and 5 h were referred to H_2O US 2 h, and H_2O US 5 h, respectively whereas the samples sonicated in hydrogen peroxide for 2 h and 5 h were referred to H_2O_2 US 2 h, and H_2O_2 US 5 h, respectively.

2.2. Laser granulometry

The particle size distribution was determined by Dynamic Light Scattering (DLS) by using a Mastersizer 2000 particle size analyzer (Malvern Instruments, range 0.02 μm to 2000 μm). Prior to analysis the samples were agitated in distilled water to ensure a good dispersion.

2.3. Adsorption experiments

The effects of time (adsorption kinetics), concentration (equilibrium experiments), temperature (adsorption isotherms), and particle size have been investigated.

The kinetic study was carried out at 25 °C. Several solutions of $Mn(NO_3)_2$ of 25 mL and initial concentration of 70 $mg \cdot L^{-1}$ were prepared. They were mixed with 125 mg of vermiculite in stoppered agitated flasks (300 rpm). The residual manganese concentration in each flask was determined after increasing contact time (between 30 min and 1300 min).

The equilibrium adsorption experiments were carried out in stoppered flasks containing 125 mg of vermiculite and 25 mL of manganese nitrate solution of concentration in the 5–300 $mg \cdot L^{-1}$ range. The measured pH of the dispersions was kept between 6.8 and 6.9. The flasks were homogenized by agitation with a magnetic stirrer (300 rpm) and immersed in a water bath at a constant temperature (25 °C or 35 °C or 45 °C) for 18 h. The vermiculite was further separated from the solution by centrifugation and the residual manganese, nitrate, potassium and calcium concentrations were measured.

The effect of particle size was studied by determining the adsorption isotherms at room temperature of the various vermiculite types (raw, milled and sonicated).

2.4. Determination of the manganese, nitrate, potassium and calcium concentrations

The remaining Mn^{2+} cations were oxidized into permanganate using potassium periodate in acidic medium according to the following reaction:

$$8\ Mn^{2+} + 5\ IO_4^- + 12\ H_2O \rightleftharpoons 8\ MnO_4^- + 5\ I^- + 24\ H^+$$

The formed permanganate anions were analyzed by UV–visible spectrophotometry (Jenway 7305) at 525 nm. The nitrate anions were treated with sodium salicylate to obtain yellow sodium paranitrosalicylate which was analyzed at 415 nm by UV–visible spectrophotometry. The potassium and calcium ions were analyzed by flame emission spectrometry (Jenway PFP7).

2.5. Thermodynamics of adsorption

The fitting of the isotherms at three different temperatures (25 °C, 35 °C and 45 °C) was tried by using the Freundlich, the Dubinin-Kaganer-Radushkevich, the Langmuir, and the Langmuir-Freundlich models, using an iterative procedure based on a non-linear least squares algorithm.

The Freundlich equation is:

$$Q_e = K_f\,(Ce)^m \tag{1}$$

where Q_e is the adsorption uptake at equilibrium ($mg\cdot g^{-1}$), C_e is the concentration at equilibrium ($mg\cdot L^{-1}$), K_f is the Freundlich constant ($L^n\cdot mg^{1-n}\cdot g^{-1}$), and m is the Freundlich exponent.

The Dubinin-Kaganer-Radushkevich equation is:

$$Q_e/Q_{max} = \exp\left(-\beta \times \left(RT \times \ln(1/Ce)^2\right)\right) \tag{2}$$

where Q_{max} is the maximum uptake ($mg\cdot g^{-1}$), β is the activity coefficient ($mol^2\cdot J^{-2}$) related to mean adsorption energy, R is the perfect gas constant ($J\cdot K^{-1}\cdot mol^{-1}$), and T is the temperature (K).

The Langmuir-Freundlich equation is:

$$Q_e/Q_{max} = \theta = (K_{lf}\,Ce)^n/(1 + (K_{lf}\,Ce)^n) \tag{3}$$

where θ is the coverage ratio, K_{lf} is the Langmuir-Freundlich constant ($L\cdot mg^{-1}$) and n is the Langmuir-Freundlich exponent.

When the Langmuir-Freundlich exponent is equal to one (n = 1), Eq. (3) becomes the Langmuir equation.

Modelling of the adsorption isotherms using the Langmuir-Freundlich equation (Yao, 2000) has allowed to determine the thermodynamic parameters of adsorption. The Gibbs free energy (ΔG°_T) was calculated according to the following equations:

$$\Delta G^\circ_T = -RT\ln(K_d) \tag{4}$$

where R (8.314 $J\cdot mol^{-1}\cdot K^{-1}$) is the perfect gas constant, T is the solution temperature (K) and K_d is the equilibrium constant.

The expression of K_d is:

$$K_d = C_a/C_e \tag{5}$$

where C_a ($mg\cdot L^{-1}$) is the solute concentration adsorbed at equilibrium ($C_a = Q_e \times m/V$, where m is the weight of adsorbent and V the total volume) and C_e is the concentration of solute remaining in the solution at equilibrium ($mg\cdot L^{-1}$).

The refined parameters of the Langmuir-Freundlich fits (Q_{max}, n and K_{lf}) were used to calculate C_e at a given value of the coverage ratio θ ($C_e = f(\theta)$) from Eq. (3). Thus, the K_d values and the adsorption isosteric Gibbs Free energy (ΔG°_T) were calculated at given θ values by using the Eqs. (5) and (4), respectively.

Thus, assuming that ΔH° and ΔS° are temperature-invariant variables:

$$\ln(K_d) = -\Delta H^\circ/RT + \Delta S^\circ/R \tag{6}$$

According to the so-called Van't Hoff method, isosteric ΔH° and ΔS° values at a given adsorption uptake were calculated at a given θ value from the slope and intercept of the plot of ln (K_d) versus 1/T.

2.6. Adsorption kinetics

Two kinetics models were applied to simulate the adsorption kinetics data in order to investigate the behaviour of adsorption process of Mn^{2+} onto vermiculite: the pseudo-first-order (Lagergren, 1898), and the pseudo-second-order (Ho and McKay, 1999).

The first-order equation is:

$$dQ_t/dt = k_1 \times (Q_e - Q_t) \tag{7}$$

where k_1 is the rate constant of pseudo-first-order adsorption (min^{-1}), Q_e and Q_t ($mg\cdot g^{-1}$) are the amounts of adsorbed manganese at equilibrium and at time t (min) respectively. k_1 and Q_e values were calculated from the non-linear regression of Q_t versus t obtained by integration of Eq. (7).

The second-order equation is:

$$dQ_t/dt = k_2 \times (Q_e - Q_t)^2 \tag{8}$$

where k_2 is the rate constant of pseudo-second-order adsorption ($g.mg^{-1}\cdot min^{-1}$), Q_e and Q_t ($mg\cdot g^{-1}$) are the amounts of adsorbed Mn^{2+} at equilibrium and at time t (min) respectively. k_2 and Q_e values were determined from the non-linear regression of Q_t versus t obtained by integration of Eq. (8).

3. Results and discussions

3.1. Manganese adsorption on raw vermiculite

3.1.1. Adsorption kinetics at 25 °C

Fig. 1 shows the kinetics of adsorption of Mn^{2+} on raw vermiculite.

The equilibrium time of adsorption was reached rapidly, i.e. after 1 h of agitation. The kinetics curve has been properly fitted by a pseudo-first-order ($R^2 = 0.9997$ and RMSE = 0.059) and a second-order model ($R^2 = 0.9998$ and RMSE = 0.046). The best fit was obtained by the pseudo second-order model (Fig. 1). In this case, the adjusted rate constant and the amount of adsorbed Mn^{2+} at equilibrium are 0.0537 $g\cdot mg^{-1}\cdot min^{-1}$and 13.92 $mg\cdot g^{-1}$, respectively.

3.1.2. Mn^{2+} adsorption mechanism (edge site adsorption versus ion exchange) at 25 °C

Fig. 2 shows adsorption isotherms of Mn^{2+} at 25 °C on raw vermiculite. Details of the amount of adsorbed (Mn^{2+}, NO_3^-) or exchanged (Ca^{2+}, K^+) ions on raw vermiculite versus Mn^{2+} initial concentration are exposed in Fig. 3.

The adsorption isotherm of manganese on raw vermiculite follows a Langmuir model with a maximum uptake of 28.34 $mg\cdot g^{-1}$ (Fig. 2) corresponding to an expected 5.14 $meq\cdot L^{-1}$ exchange capacity. The theoretical cationic exchange capacity (CEC) of this vermiculite (which corresponds to the ratio of K^+ and Ca^{2+} exchangeable cations in meq

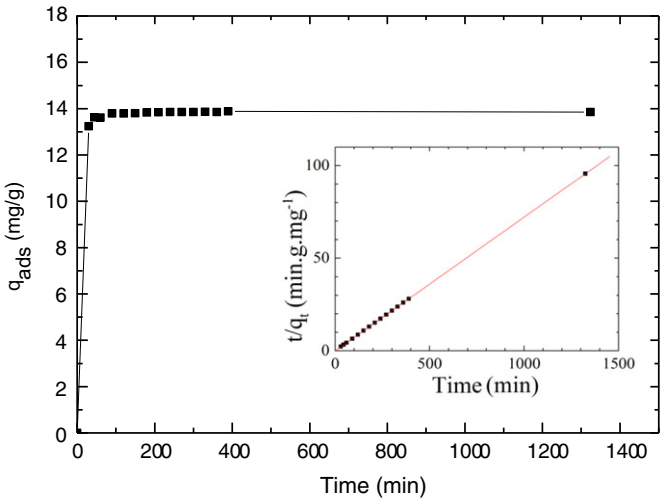

Fig. 1. Kinetic of adsorption of Mn^{2+} on raw vermiculite.

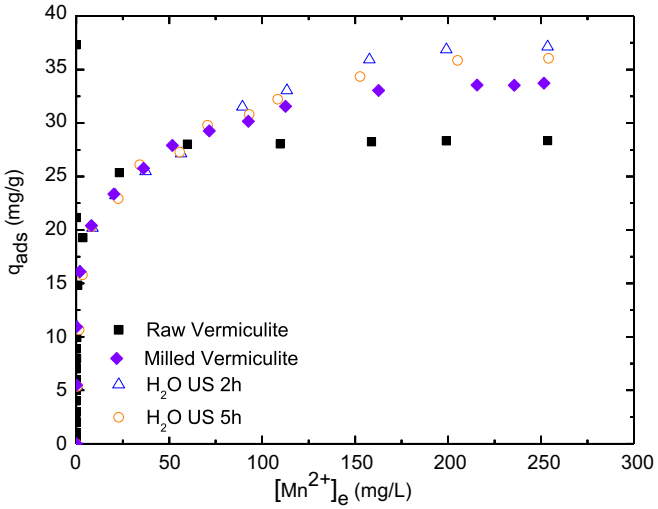

Fig. 2. Adsorption isotherms of Mn^{2+} at 25 °C on raw, milled and sonicated vermiculite (in H_2O for 2 h and 5 h).

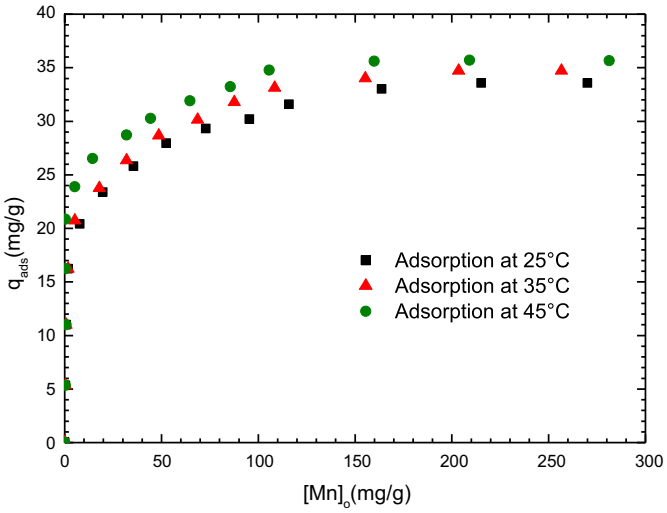

Fig. 4. Mn^{2+} adsorption isotherms of milled vermiculite at 25 °C, 35 °C and 45 °C.

to the mass of vermiculite in g), calculated from the average chemical composition is of 1.48 meq·g^{-1}. In our conditions, this CEC value corresponds to a 7.43 meq·L^{-1} exchange capacity, as CEC (meq·L^{-1}) = CEC (meq·g^{-1}) × m (g) / V (L), with V = 25 mL and m = 125 mg. Hence, the vermiculite contains enough exchangeable cations that could be exchanged with the adsorbed manganese. In this case, the amount of adsorbed manganese cations would thus be equal to the sum of the exchanged Ca^{2+} and K^+ ions (in equivalent per liter or per gram). However, the total amount of K^+ and Ca^{2+} exchanged ions analyzed after the adsorption experiment was quite lower than adsorbed manganese ions (Fig. 3). For example, the concentration of Ca^{2+} and K^+ ions released in the solution at equilibrium is only of 0.75 meq·$L^{-1}$and 0.136 meq·L^{-1}, respectively (Fig. 3), which represents a total quantity of 0.886 meq·L^{-1}. This latter value is lower than the total amount of Mn^{2+} removed by the vermiculite (i.e. 5.14 meq·L^{-1}) which means that only few Mn^{2+}cations have been exchanged (about 17%) but that these cations have mainly been adsorbed (83%) at the edges of the layers.

As clearly explained in the litterature, vermiculite is capable to adsorb heavy metals via two different mechanisms: (1) by exchanging its cations at the planar sites, resulting from interactions between the metallic ions and its negative permanent charge (outer-sphere complexes) (Walker, 1950) and (2) by formation of inner-sphere complexes through Si—O— and Al—O— groups at the clay mineral particle's edges (Adebowale et al., 2005; Angove et al., 1997; Kraepiel et al., 1999; Mercier and Detellier, 1995; Naseem and Tahir, 2001; Sari et al., 2007).

The amount of NO_3^- ions adsorbed by raw vermiculite at equilibrium (i.e. 4.50 meq·L^{-1}, Fig. 3) was almost equal to the amount of Mn^{2+} ions adsorbed at the edge of the layers (4.25 meq·L^{-1}). The similar profile of the NO_3^- and Mn^{2+} adsorption curves (Fig. 3) suggests that the adsorption of both species occurs simultaneously. Moreover, the adsorption of these ions starts at the same time and at very low concentration (Fig. 3). On the contrary, the ion exchange of K^+ and Ca^{2+} is almost not observed at very low Mn^{2+} concentration (Fig. 3, less than 4 meq·L^{-1}). Thus, the first adsorption sites of Mn^{2+} (for low adsorbate concentration) are expected to be some coordination sites: Si—O or Al—O sites present at the edge of the layers, possibly because these edge sites are easier to access by external mass transfer.

The fact that almost one milli-equivalent of NO_3^- anion is adsorbed per one milli-equivalent of Mn^{2+} cation suggests that each Mn^{2+} cation is complexed both by coordination with the oxygen atoms from the Si—O or Al—O layer edge groups but also by one nitrate ion. The pH of the vermiculite dispersion in our conditions was about 6.9. It was shifted to 6.5 after adsorption of Mn^{2+} (initial concentration of

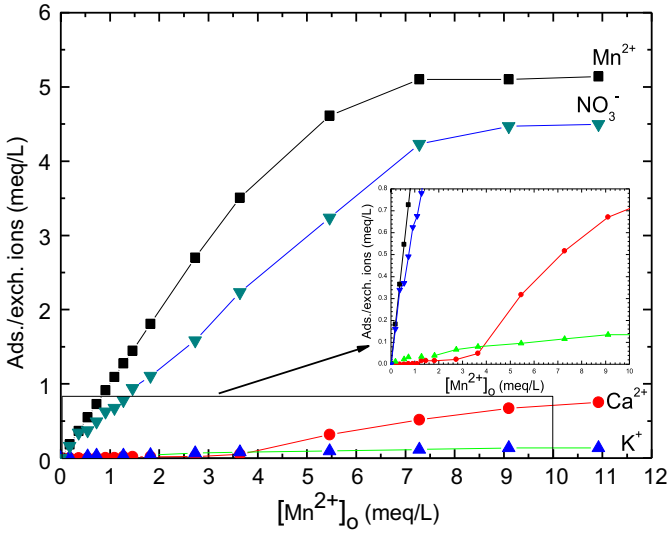

Fig. 3. Evolution of the amount of adsorbed (Mn^{2+}, NO_3^-) or exchanged (Ca^{2+}, K^+) ions on raw vermiculite, during the adsorption of Mn^{2+} at different initial concentrations.

Table 1
Parameters of the Langmuir –Freundlich fitting of the Mn^{2+} adsorption isotherms.

T °C	Q_{max} ($mg \cdot g^{-1}$)	K_{lf} ($L \cdot mg^{-1}$)	n	R^2	RMSE
25	83.12	7.576×10^{-4}	0.2129	0.9027	3.730
35	61.98	1.251×10^{-2}	0.2623	0.9141	3.672
45	163.9	1.491×10^{-7}	0.1228	0.9114	3.572

300 ppm), indicating that no protons were released in the solution after the adsorption of Mn^{2+} (delta$[H^+] = 10^{-6.5}$–$10^{-6.9} = 1.9.10^{-7}$ mol·L^{-1}, which is negligible). Thus, the electro-neutrality of the solution was maintained by the coadsorption of NO_3^- with Mn^{2+}.

Fig. 3 also shows that the interlayer K^+ ions are primarily exchanged at low concentrations while the Ca^{2+} ones are only released for a Mn^{2+} concentration above 3 meq·L^{-1}. The easier K^+ exchange compared to the Ca^{2+} one at low concentration could be attributed to a lower attraction force for the potassium with respect of the negatively charged layers owing to its lower charge (single charge of K^+ versus double charge of Ca^{2+}). However, above 5 meq·L^{-1}, the quantity of exchanged Ca^{2+} becomes dominating. This result is in agreement with the work of Monsef-Mirzai and Mc Whinnie (Monsef-Mirzai and Mc Whinnie, 1983) who reported that the exchangeable cations were released in the order $Ca^{2+} > Mg^{2+} > Na^+ > K^+$, for the adsorption of copper (II) on a montmorillonite. Indeed, it is well known that the exchanged K^+ cations in vermiculite are dehydrated and well retained in the hexagonal cavities due to their appropriate ionic radius which is close to the cavity radius (Barshad, 1954; Barshad and Kishk, 1970; Dolcater et al., 1972). The K^+ vermiculite has a d(001) spacing of 1 nm, hindering the cation exchange while the presence of Ca^{2+} cations yields to expanded d(001) spacing of 1.2 nm. Thus, the Ca^{2+} cations are expected to be easier exchanged in vermiculite than the K^+ ones. In our case, the amounts of exchanged Ca^{2+} and K^+ ions were of 0.75 meq·L^{-1} and 0.136 meq·L^{-1}, respectively, for raw vermiculite containing about five times less interlayer calcium than potassium, as explained in section 2.1. This result confirms the greater amount of Ca^{2+} exchanged.

At equilibrium, only 17% (in equivalent) of the total adsorbed Mn^{2+} amount have been exchanged: 14% were exchanged against Ca^{2+} ionsand 3% against K^+ ions. The Mn^{2+} cations have been mainly adsorbed (83%) at the edges of the layers together with the NO_3^- ions.

3.2. Temperature effect of the manganese adsorption on milled vermiculite

Fig. 4 shows the adsorption isotherms of Mn^{2+} on the milled vermiculite at three temperatures: 25 °C, 35 °C and 45 °C.

Neither the Langmuir model nor the Dubinin-Kaganer-Radushkevich one allows a satisfying fit of the adsorption isotherms. Indeed, for the Langmuir model fitting of the isotherms at 25 °C, 35 °C and 45 °C, R^2 values are 0.8489, 0.8787 and 0.869, respectively. For the Dubinin-Kaganer-Radushkevich model fitting of the isotherms at 25 °C, 35 °C and 45 °C, R^2 values are 0.4325, 0.2481 and 0.3862, respectively.

The manganese adsorption isotherms on the milled vermiculite have also been fitted by the Langmuir-Freundlich and the Freundlich models (Table 1 and Table 2) which can better represent the experimental data. The temperature has little influence on the adsorption equilibrium (Fig. 4). A small increase in the manganese adsorption was underlined

Table 2
Parameters of the Freundlich fitting of the Mn^{2+} adsorption isotherms.

T °C	K_f ($L^n \cdot mg^{1-n} \cdot g^{-1}$)	m	R^2	RMSE
25	15.51	0.1453	0.9022	3.580
35	16.13	0.1465	0.9127	3.545
45	20.83	0.1021	0.9252	3.417

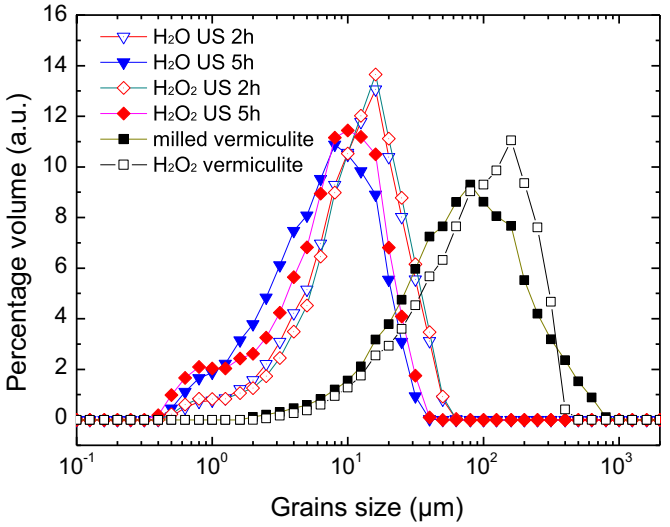

Fig. 5. Effect of the ultrasonic treatment on the granulometry of milled vermiculite, vermiculite treated in H_2O_2 for 5 h and treated under ultrasounds either in H_2O or H_2O_2 (for 2 h and 5 h).

with increasing temperature, which indicates an endothermic adsorption process. The Gibbs free energy at 298 K ($\Delta G°_{298}$) determined according to Eq. (4) at a coverage ratio $\theta = 0.9$ is equal to -0.6 kJ·mol^{-1} indicating that the adsorption process is spontaneous. The enthalpy and entropy variations at 298 K ($\Delta H°_{298}$ and $\Delta S°_{298}$) at $\theta = 0.9$ calculated from the Van't Hoff method (Section 2.5) are 34 kJ·mol^{-1} and 116 J·K^{-1}.mol^{-1}, respectively. The values are in agreement with an adsorption promoted by an entropy increase which could be due to a removal of the water molecules adsorbed at the edges of the layers as they would be replaced by manganese cations and nitrate anions. As explained, the manganese cations and nitrate anions could have formed some inner-sphere complexes in the absence of water between the adsorbate and the surface functional group (Goldberg, 2005).

3.3. Effect of size reduction on the manganese removal

Fig. 5 shows the granulometry distribution of milled vermiculite dispersions prior and after ultrasonic treatment in water or hydrogen

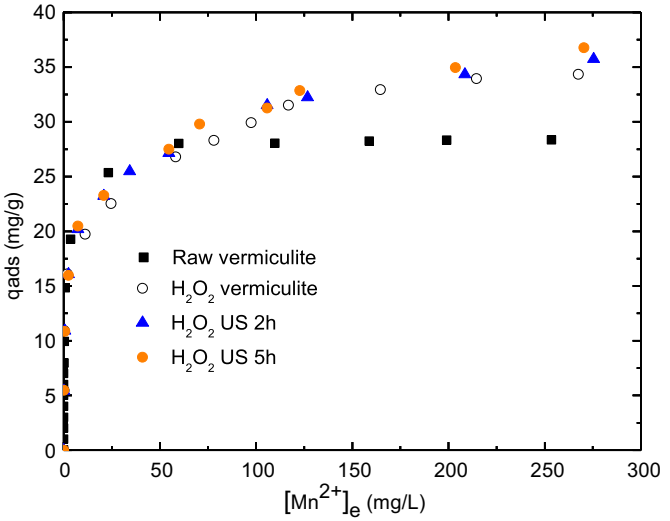

Fig. 6. Mn^{2+} adsorption isotherms on raw, milled, H_2O_2 treated and H_2O_2 sonicated vermiculites (for 2 h and 5 h).

Table 3
Relation between the structural parameters (particle size mode, one-fourth of the sum of perimeters) and the manganese adsorption capacity.

Sample type	Maximum uptake Q_{ads} ($mg \cdot g^{-1}$)	Particle size mode L (μm)	L_0/L (μm) with L_0 = 77 μm	One-fourth of the sum of perimeters $L_0 \times \{\{\text{integer part } (L_0/L)\} + 1\}$ (μm)
Milled vermiculite	33.73	77	–	77
H_2O_2 sonicated vermiculite (2 h)	35.74	13.2	5.83	462
H_2O sonicated vermiculite (2 h)	36.06	12.7	6.06	539
H_2O_2 sonicated vermiculite (5 h)	36.77	10.2	7.55	616
H_2O sonicated vermiculite (5 h)	37.13	8.7	8.85	693

peroxide (for 2 h and 5 h). The adsorption isotherms of Mn^{2+} on the raw and milled vermiculite were compared either to H_2O sonicated, H_2O_2 treated and H_2O_2 sonicated samples, as seen in Fig. 2 and Fig. 6.

The reduction of the particle size is known to yield to a slight increase in specific surface area (Pérez-Maqueda et al., 2004; Nguyen et al., 2013). For vermiculite, size reduction can be achieved by sonication as this treatment is known to preserve its crystalline structure (Nguyen et al., 2013; Ali et al., 2014). The particles of raw vermiculite were thus broken by conventional milling and sonication in order to generate new layer edges. By conventional milling, reduced sizes in the 2 μm–800 μm range were obtained, with a mode at 77 μm (Fig. 5). The adsorption isotherm of Mn^{2+} by milled vermiculite (Fig. 2) shows a maximum adsorption capacity of 33.73 $mg \cdot g^{-1}$ which represents a 18% increase compared to raw vermiculite (28.32 $mg \cdot g^{-1}$). Indeed, the effect of the conventional milling is a rise in the edge adsorption site content that increases the Mn^{2+} adsorption capacity of vermiculite (Fig. 2).

To enhance this effect, the particle size of the vermiculite was again reduced by sonication (Reinholdt et al., 2013; Kehal et al., 2010; Küncek and Sener, 2010) of dispersions in water for 2 h, giving a size distribution centered at 16 μm (Fig. 5). Increasing the sonication time from 2h to 5h involved a slight reduction in the size of the particles, yielding an asymmetrical bimodal size distribution with a main mode at 8 μm and a minor one at 0.8 μm. In this case, the reduction in the particle size is very effective to create new edge sites yielding to a rise in the maximum uptake of adsorbed Mn^{2+} by vermiculite (37.13 $mg \cdot g^{-1}$), which represents an increase of 31% compared to raw vermiculite (Fig. 2).

To increase the size reduction, the vermiculite particles were also sonicated in a 35% hydrogen peroxide solution. The decomposition of H_2O_2 is known to release dioxygen gas within the interlayer spacing of vermiculite, thus exfoliating its layers (Groves, 1939). The Mn^{2+} adsorption uptake of the milled vermiculite chemically exfoliated in hydrogen peroxide (Q_{ads} = 34.3 $mg \cdot g^{-1}$) is marginally higher than the pristine milled vermiculite (Q_{ads} = 33.73 $mg \cdot g^{-1}$). For this former sample (referred to H_2O_2 vermiculite), the exfoliation did not have any effect on the adsorption uptake compared to milled vermiculite (Figs 2 and 6) because it has separated the layers and increased the specific surface area without creation of new edge sites needed for the Mn^{2+} adsorption. The effect of H_2O_2 addition during the sonication appears to be negligible for processing times less than 2 h, giving quite similar particle size distribution than the one obtained by sonication in pure water (Fig. 5). After 5 h of ultrasound irradiation, the particle size distribution is also bimodal with a minor mode at 0.8 μm, as the distribution of the particles sonicated for the same time in water (Fig. 5). The sonication in hydrogen peroxide resulted in an increase in the maximum adsorption uptake of 26% and 30% compared to raw vermiculite for 2 h and 5 h of treatment, respectively.

Assuming that the adsorption process of Mn^{2+} is mainly controlled by the chemisorption on the edge of the layers, the increase in the maximum uptake of adsorbed Mn^{2+} might be proportional to the average perimeter of the particles. This perimeter can be calculated by assuming that the pristine particles are in the form of squares of L_0 side dimension. They can be splitted through ultrasounds in multiple smaller particles also of square shape and L side dimension. The number of small particles is $(L_0/L)^2$ if L_0/L is an integer (see Fig. 1 in background dataset). Thus the sum of the side dimensions of the small splitted particles (i.e the one-fourth of the sum of the perimeters.) is equal to $(L_0)^2/L$.

If the $(L_0)/L$ value is not an integer (see Fig. 2 in background dataset), the sonication splitting yields to the formation of n^2 square particles of L side dimension (n = {integer part (L_0/L)}), one square particle of {{decimal part (L_0/L)} × L} side dimension, and 2n rectangle particles (which perimeter is equal to 2 × {L + {decimal part (L_0/L)} × L}). In this latter case, a simplified calculation of the one-fourth of the sum of the small particle perimeters gives $L_0 \times \{\{\text{integer part } (L_0/L)\} + 1\}$.

The average size dimension (L) of one kind of particle distribution has been assumed to be equal to the value of the statistics mode of the particle distribution size (values in Table 3). The L_0 dimension size of the pristine grinded vermiculite (which was splitted in other particle distribution by ultrasonic treatment) is equal to 77 μm. The plot of the Mn^{2+} maximum adsorption uptake versus the sum of the one-fourth perimeters of the splitted particles (Table 3) is linear (Fig. 7) with a R^2 linear correlation coefficient of 0.9927. This result is in agreement with an adsorption process at the edge of the layers of the particles.

4. Conclusion

For large size vermiculite, the adsorption equilibrium has been attained after a contact time of one hour and the phenomenon is endothermic. Namely, the increase in the temperature between 25 °C and 45 °C slightly increased the adsorbed manganese amount. The Mn^{2+} adsorption capacity on the raw vermiculite is about 28.32 $mg \cdot g^{-1}$. The adsorption mechanism is mainly governed by a complexation of the manganese at the edges of the layers (about 83%) and marginally by a cationic exchange (about 17%). The NO_3^- anions have been co-adsorbed with the complexed Mn^{2+} at the edge of the layers and this

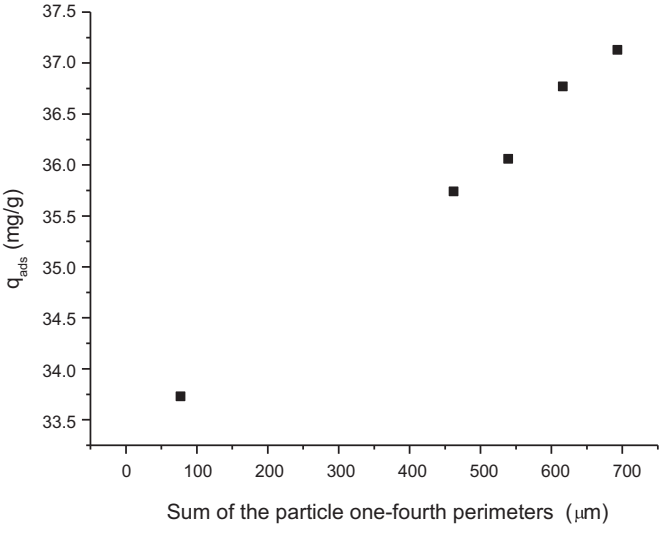

Fig. 7. Mn^{2+} maximum adsorption uptake as a function of the sum of the one-fourth perimeters of the particles $L_0 \times \{\{\text{integer part } (L_0/L)\} + 1\}$, where L_0 and L are the average dimension sizes of the milled vermiculite (77 μm) and of the particles obtained from milled vermiculite by sonication in water or H_2O_2.

fact suggests that $[MnNO_3]^+$ cations have been coordinated with the oxygen atoms from the Si—O or Al—O groups at the edges of the layers.

The reduction of the particle size of vermiculite by mechanical milling, sonication of vermiculite dispersions in 35% hydrogen peroxide and ultrasound irradiation at 20 kHz of aqueous vermiculite dispersion for 5 h increased the adsorption capacity to 33.73, 36.77 and 37.13 $mg \cdot g^{-1}$, respectively. The effect of sonication milling is a decrease in the particle size which generates higher amount of the edge adsorption sites. Thus, the adsorption capacity of Mn^{2+} was proportional to the sum of the estimated geometric perimeter of the particles assuming square shaped particles.

Appendix A. Supplementary data

Supplementary data to this article can be found online at http://dx.doi.org/10.1016/j.clay.2016.12.041.

References

Adebowale, K.O., Unuabonah, I.E., Olu-Owolabi, B.I., 2005. Adsorption of some heavy metal ions on sulfate- and phosphate-modified kaolin. Appl. Clay Sci. 29 (2), 145–148.

Akpomie, K.G., Dawodu, F.A., 2014. Efficient abstraction of nickel(II) and manganese(II) ions from solution onto an alkaline-modified montmorillonite. J. Taibah Univ. Sci. 8, 343–356.

Ali, F., Reinert, L., Levêque, J.M., Duclaux, L., Muller, F., Saeed, S., Shah, S.S., 2014. Effect of sonication conditions: solvent, time, temperature and reactor type on the preparation of micron sized vermiculite particles. Ultrason. Sonochem. 21, 1002–1009.

Angove, M.J., Johnson, B.B., Wells, J.D., 1997. Adsorption of cadmium(II) on kaolinite. Colloids Surf. A Physicochem. Eng. Asp. 126 (2–3), 137–147.

Ates, A., Akgül, G., 2016. Modification of natural zeolite with NaOH for removal of manganese in drinking water. Powder Technol. 287, 285–291.

Barshad, I., 1954. Cation exchange in micaceous minerals: II. replaceability of ammonium and potassium from vermiculite, biotite, and montmorillonite. Soil Sci. 78 (1), 57–76.

Barshad, I., Kishk, F.M., 1970. Factors affecting potassium fixation and cation exchange capacities of soil vermiculite clays. Clay Clay Miner. 18, 127–137.

Da Fonseca, M.G., De Oliveira, M.M., Arakaki, L.N.H., 2006. Removal of cadmium, zinc, manganese and chromium cations from aqueous solution by a clay mineral. J. Hazard. Mater. B137, 288–292.

Dawodu, F.A., Akpomie, K.G., 2014. Simultaneous adsorption of Ni(II) and Mn(II) ions from aqueous solution unto a Nigerian kaolinite clay. J. Mater. Res. Technol. 3 (2), 129–141.

Dolcater, D.L., Jackson, M.L., Syers, J.K., 1972. Cation exchange selectivity in mica and vermiculite. Am. Mineral. 57, 1823–1831.

Dzene, L., Tertre, E., Hubert, F., Ferrage, E., 2015. Nature of the sites involved in the process of cesium desorption from vermiculite. J. Colloid Interface Sci. 455, 254–260.

Goldberg, S., 2005. Inconsistency in the triple layer model description of ionic strength dependent boron adsorption. J. Colloid Interface Sci. 285, 509–517.

Groves, R.C., 1939. Exfoliation of vermiculite by chemical means. Nature 144 (3647), 554.

Ho, Y.S., McKay, G., 1999. Pseudo-second order model for sorption processes. Process Biochem. 34, 451–465.

Hua, M., Zhang, S., Pan, B., Zhang, W., Lv, L., Zhang, Q., 2012. Heavy metal removal from water/wastewater by nanosized metal oxides: a review. J. Hazard. Mater. 211–212, 317–331.

Jimenez de Haro, M.C., Martinez Blanes, J.M., Poyato, J., Pérez-Maqueda, L.A., Lerf, A., Pérez-Rodriguez, J.L., 2004. Effect of mechanical treatment and exchanged cation on the micro porosity of vermiculite. J. Phys. Chem. Solids 65, 435–439.

Jusoh, A., Cheng, W.H., Low, W.M., Nora'aini, A., Megat Mohd Noor, M.J., 2005. Study on the removal of iron and manganese in groundwater by granular activated carbon. Desalination 182 (1–3), 347–353.

Kehal, M., Reinert, L., Duclaux, L., 2010. Characterization and boron adsorption capacity of vermiculite modified by thermal shock or H_2O_2 reaction and/or sonication. Appl. Clay Sci. 48, 561–568.

Kraepiel, A.M.L., Keller, K., Morel, F.M.M., 1999. A model for metal adsorption on montmorillonite. J. Colloid Interface Sci. 210 (1), 43–54.

Krauss, G., 2005. Steels: Processing, Structure, and Performance. ASM International (613 pp).

Küncek, I., Sener, S., 2010. Adsorption of methylene blue onto sonicated sepiolite from aqueous solutions. Ultrason. Sonochem. 17, 250–257.

Lagaly, G., Ogawa, M., Dékány, I., 2006. In: Bergaya, F., Theng, B.K.G., Lagaly, G. (Eds.), Handbook of Clay Science. Elsevier, Amsterdam.

Lagergren, S., 1898. Zur theorie der sogenannten adsorption gel sterstöffe. Kungliga Svenska Vetenskapsakademiens Handlingar 24, 1–39.

Malandrino, M., Abollino, O., Giacomino, A., Aceto, M., Mentasti, E., 2006. Adsorption of heavy metals on vermiculite: influence of pH and organic ligands. J. Colloid Interface Sci. 299, 537–546.

Mercier, L., Detellier, C., 1995. Preparation, characterization, and applications as heavy metals sorbents of covalently grafted thiol functionalities on the interlamellar surface of montmorillonite. Environ. Sci. Technol. 29 (5), 1318–1323.

Monsef-Mirzai, P., Mc Whinnie, W.R., 1983. Transition metal ion (Cu^{2+}, Mn^{2+}, VO^{2+})-montmorillonite interactions. Inorg. Chim. Acta 73, 41–44.

Naseem, R., Tahir, S.S., 2001. Removal of Pb(II) from aqueous/acidic solutions by using bentonite as an adsorbent. Water Res. 35 (16), 3982–3986.

Nguyen, A.N., Reinert, L., Leveque, J.M., Beziat, A., Dehaudt, P., Juliaa, J.F., Duclaux, L., 2013. Preparation and characterization of micron and submicron-sized vermiculite powder by ultrasonic irradiation. Appl. Clay Sci. 72, 9–17.

Olsen, S.E., Olsen, S., Tangstad, M., Lindstad, T., 2007. Production of Manganese Ferroalloys. Tapir Academic Press (247 pp).

Patil, D.S., Chavan, S.M., Kennedy Oubagaranadin, J.U., 2016. A review of technologies for manganese removal from wastewaters. J. Environ. Chem. Eng. 4, 468–487.

Pérez-Maqueda, L.A., Caneo, O.B., Poyato, J., Perez-Rodriguez, J.L., 2001. Preparation and characterization of micron and submicron-sized vermiculite. Phys. Chem. Miner. 28, 61–66.

Pérez-Maqueda, L.A., Jiménez de Haro, M.C., Poyato, J., Pérez-Rodríguez, J.L., 2004. Comparative study of ground and sonicated vermiculite. J. Mater. Sci. 39, 5347–5351.

Perez-Rodriguez, J.L., Carrera, F., Poyato, J., Perez-Maqueda, L.A., 2002. Sonication as a tool for preparing nanometric vermiculite particles. Nanotechnology 13, 382–387.

Pfeifer, G.D., Roper, J.M., Dorman, D., Lynam, D.R., 2004. Health and environmental testing of manganese exhaust products from use of methylcyclopentadienyl manganese tricarbonyl in gasoline. Sci. Total Environ. 334–335, 397–408.

Poyato, J., Perez-Rodriguez, J.L., Ramirez-Valle, V., Lerf, A., Wagner, F.E., 2009. Sonication induced redox reaction of the Ojen (Andalucia, Spain) vermiculite. Ultrason. Sonochem. 16, 570–576.

Reinholdt, M.X., Hubert, F., Faurel, M., Tertre, E., Razafitianamaharavo, A., Francius, G., Prêt, D., Petit, S., Béré, E., Pelletier, M., Ferrage, E., 2013. Morphological properties of vermiculite particles in size-selected fractions obtained by sonication. Appl. Clay Sci. 77–78, 18–32.

Sari, A., Tuzen, M., Citak, D., Soylak, M., 2007. Equilibrium, kinetic and thermodynamic studies of adsorption of Pb(II) from aqueous solution onto Turkish kaolinite clay. J. Hazard. Mater. 149 (2), 283–291.

Spinti, M., Zhuang, H., Trujillo, E.M., 1995. Evaluation of immobilized biomass beads for removing heavy metals from wastewaters. Water Environ. Res. 67 (Number 6), 943–952.

Valaškova, M., Simha Martynkova, G., 2012. Vermiculite: structural properties and examples of the use. In: Valaškova, M., Simha Martynkova, G. (Eds.), Clay Minerals in Nature–Their Characterization, Modification and Application. InTech, pp. 209–238.

Walker, G.F., 1950. Trioctahedral minerals in the soil-clays of north-east Scotland. Min. Mag. 29, 72–84.

WHO, 2011. Manganese in drinking-water. Background Document for Preparation of WHO Guidelines for Drinking-water Quality. World Health Organization, Geneva (WHO/SDE/WSH/03.04/104/Rev/1).

Wiewiora, A., Perez-Rodriguez, J.L., Perez-Maqueda, J.L., Drapala, J., 2003. Particle size distribution in sonicated high- and low- charge vermiculites. Appl. Clay Sci. 24, 51–58.

Yao, C., 2000. Extended and improved Langmuir equation for correlating adsorption equilibrium data. Sep. Purif. Technol. 19, 237–242.